Geochemistry Geophysics Geosystems G3
AN ELECTRONIC JOURNAL OF THE EARTH SCIENCES
Published by AGU and the Geochemical Society

Article
Volume 9, Number 11
19 November 2008
Q11U02, doi:10.1029/2008GC002096
ISSN: 1525-2027

Detrital input, productivity fluctuations, and water mass circulation in the westernmost Mediterranean Sea since the Last Glacial Maximum

F. J. Jimenez-Espejo
Institute for Research on Earth Evolution, Japan Agency for Marine-Earth Science and Technology, Natsushima-cho 2-15, Yokosuka, 237-0061, Japan (fjjspejo@jamstec.go.jp)

F. Martinez-Ruiz
Facultad de Ciencias, Instituto Andaluz de Ciencias de la Tierra, Campus Fuentenueva, E-18002 Granada, Spain

M. Rogerson
Department of Geography, University of Hull, Cottingham Road, Hull HU6 7RX, UK

J. M. González-Donoso
Departamento de Ecología y Geología, Universidad de Málaga, Campus de Teatinos, s/n, E-29071, Málaga, Spain

O. E. Romero
Facultad de Ciencias, Instituto Andaluz de Ciencias de la Tierra, Campus Fuentenueva, E-18002 Granada, Spain

D. Linares
Departamento de Ecología y Geología, Universidad de Málaga, Campus de Teatinos, s/n, E-29071, Málaga, Spain

T. Sakamoto
Program for Paleoenvironment, Institute for Research on Earth Evolution, Japan Agency of Marine-Earth Science and Technology, Natsushima-cho 2-15, Kita-ku, Yokosuka, Kanagawa 237-0061, Japan

D. Gallego-Torres
Departamento de Mineralogía y Petrología, Facultad de Ciencias, Universidad de Granada, IACT, Campus Fuentenueva, Granada E-18002, Spain

J. L. Rueda Ruiz
Departamento de Ecología y Geología, Universidad de Málaga, Campus de Teatinos, s/n, E-29071, Málaga, Spain

M. Ortega-Huertas
Departamento de Mineralogia y Petrologia, Facultad de Ciencias, Universidad de Granada, Campus Fuentenueva, Granada E-18002, Spain

J. A. Perez Claros
Departamento de Ecología y Geología, Universidad de Málaga, Campus de Teatinos, s/n, E-29071, Málaga, Spain

[1] By presenting sea surface temperatures, planktonic oxygen isotope profiles, and bulk geochemical composition of core sediments, we offer a multiparameter reconstruction of Western Mediterranean oceanography from the Last Glacial Maximum until the Middle Holocene (20,000–5000 cal years B. P.). Sediments from Ocean Drilling Program Site 975 in the Algero-Balearic basin have been compared with

three Alboran basin cores (TTR-300G, TTR-302G, and TTR-304G), all of them investigated at high resolution. This multiproxy approach has allowed two different modes of circulation to be recognized: (1) during the LGM and from ~8.0 cal. ka B. P. onward, no surface gradient in $\delta^{18}O_{G.\ bulloides}$ is found associated with low productivity, in close analogy to modern conditions; (2) during the Bølling-Allerød and early Holocene, significant surface isotopic gradients are found with periods probably indicating an unstable water column, associated with enhanced productivity and low bottom oxygen conditions. The close synchrony between the occurrence of the surface isotopic offset and organic rich layer formation implicates that the origin of these features is linked, probably via shoaling of the regional thermohaline circulation. Paleo-SSTs, derived from planktonic foraminifer assemblages, indicate abrupt changes in surface conditions during the analyzed time interval. Fluctuations in marine productivity based on Ba and total organic carbon are related to water column stability and atmospheric conditions. A sharp warming and $\delta^{18}O_{G.\ bulloides}$ excursion at the end of the Younger Dryas is probably linked to glacial meltwater influence. The riverine input has been reconstructed using the Mg/Al ratio, and Mg/Al peaks during arid periods (Greenland Stadial-2a and Younger Dryas) related to "bypass" margin processes.

Components: 11,610 words, 4 figures, 3 tables.

Keywords: paleoceanography; paleoproductivity; stable isotopes; Alboran front; Holocene/Last Glacial Maximum; ODP 975B.

Index Terms: 0473 Biogeosciences: Paleoclimatology and paleoceanography (3344, 4900); 1065 Geochemistry: Major and trace element geochemistry; 3030 Marine Geology and Geophysics: Micropaleontology (0459, 4944).

Received 14 May 2008; **Revised** 22 August 2008; **Accepted** 16 September 2008; **Published** 19 November 2008.

Jimenez-Espejo, F. J., et al. (2008), Detrital input, productivity fluctuations, and water mass circulation in the westernmost Mediterranean Sea since the Last Glacial Maximum, *Geochem. Geophys. Geosyst.*, *9*, Q11U02, doi:10.1029/2008GC002096.

Theme: Circum-Iberia Paleoceanography and Paleoclimate: What Do We Know?
Guest Editors: F. Abrantes, M. Fernanda Sanchez-Gozi, C. Ruehlemann, and A. Voelker

1. Introduction

[2] Extensive paleoclimatic research in the Mediterranean during the last few decades has demonstrated the exceptional nature of Mediterranean records for paleoceanographic and paleoclimatic reconstructions at regional and global scale [e.g., *Cacho et al.*, 2006; *Colmenero-Hidalgo et al.*, 2004; *Emeis et al.*, 2000; *Krijgsman*, 2002; *Martrat et al.*, 2004; *Sierro et al.*, 2005]. Of particular importance is that high sedimentation rates in several regions have allowed records of climate variability to be developed at sufficiently high resolution to reveal millennial and even centennial-scale oscillations [e.g., *Moreno et al.*, 2005]. The Alboran Sea basin is one such case, where elevated detrital supply has resulted in exceptional marine sediment archives. Moreover, the Alboran Sea is the transition zone between Atlantic- and Mediterranean-type water [*Millot*, 1987, 1999] and strong vertical and horizontal hydrological gradients are present as a consequence. The persistence of these gradients from the Gulf of Cadiz through to the Tyrrhenian Sea on 10^4–10^5 year timescales has been documented in terms of sea surface temperatures (SSTs) and isotope records [*Cacho et al.*, 2001]. Small local or regional changes in climate are thus anticipated to be amplified in the Alboran Sea paleorecord via their impact on hydrographic conditions in the surface layer. The connection of the Alboran Sea with the NE Atlantic through the Strait of Gibraltar adds further interest to this region, as saline Mediterranean Outflow Water (MOW) may significantly affect North Atlantic circulation, and thus global climate [*Llave et al.*, 2006; *Rogerson et al.*, 2005, 2006; *Sierro et al.*, 2005; *Voelker et al.*, 2006].

[3] Though a large set of paleoclimate data is available for the region, many aspects of the paleoceanographic evolution of the western Mediterranean since the Last Glacial Maximum (LGM) remains controversial; e.g., the precise influence of Atlantic waters on past circulation in the Mediterranean, spatial and temporal importance of marine

productivity fluctuations, and the role of fresh water in these semienclosed basins. It is in this context that this paper attempts to reconstruct detrital supply, marine productivity variations, and fluvial/meltwater influence in the western Mediterranean through the last deglaciation, thus improving our understanding of the western Mediterranean Sea (WMS) past oceanography. In pursuit of this objective, a multiproxy approach has been taken in four selected marine records from the Alboran Sea and Algero-Balearic basins. The reconstruction of climatic variability and climatic/oceanographic responses has been made as follows: stable isotope (C and O) composition in *Globigerina bulloides* has been used as a proxy of sea surface conditions, while modern analog techniques (MAT) in planktonic foraminifer assemblages were applied to calculate paleo-sea surface temperatures (SSTs). Mineral and chemical composition of the studied sediments reveals sedimentary regime conditions. In particular, certain trace and major element ratios to Al are used as detrital proxies, such as Mg/Al, Si/Al, Zr/Al, K/Al. Organic matter content and composition in terms of carbon and nitrogen, as well as Ba_{excess} and marine barite, have been used as paleoproductivity proxies [*Paytan and Griffith*, 1997].

2. Oceanographic Setting

[4] The Alboran basin is surrounded by abrupt physiography drained by mountain rivers. Despite the relatively small size of these river basins, recent studies indicate that these rivers are highly important as sediment feeders to the marine environment, and in promoting flood events that result in large suspended plumes dispersed along the Alboran Sea [e.g., *Liquete et al.*, 2005; *Lobo et al.*, 2006]. In contrast, the Algero-Balearic basin is more isolated from direct continental/river discharge and from tectonic activity, the supply of the coarse fraction being dominated by atmospheric dust input, transportation via submarine canyons, and transport within bottom water masses [e.g., *Zuñiga et al.*, 2008].

[5] The surface water of the WMS is composed of inflowing (west to east) Atlantic water which is progressively modified by air-sea interaction, thus giving rise to Modified Atlantic Water (MAW) [*Millot*, 1999]. It is the distribution of this relatively cold, lower salinity, nutrient-rich Atlantic water and the rate and nature of its transformation to MAW that provides the primary control on surface water gradients in the WMS. Intermediate waters flow below the MAW in the opposite direction (east to west), and are mainly composed of the Levantine Intermediate Water (LIW) generated in the East Mediterranean Sea (EMS) [*Bryden and Stommel*, 1982]. The deepest levels are filled with Western Mediterranean Deep Water (WMDW), which is formed via deep convection in the Gulf of Lion [*Benzohra and Millot*, 1995] (Figures 1a and 1b).

[6] Secondary control on hydrography is imposed by the local wind field. Investigation of subannual changes in flow through the Strait of Gibraltar indicates that it is modulated by wind forcing [*García Lafuente et al.*, 2002], which also regulates the formation of gyres within the Alboran Sea [*Bucca and Kinder*, 1984] and transportation of atmospheric dust and moisture [*Rodriguez et al.*, 2001], thus providing the dominant control on the balance of aeolian and river sediment input to both basins. The regional wind field is a direct consequence of atmospheric pressure differences between the Mediterranean and the Gulf of Cadiz [e.g., *García Lafuente et al.*, 2002]. High atmospheric pressures in the Mediterranean promote easterly winds and vice versa for lower atmospheric pressures in the Mediterranean [*Macías et al.*, 2008]. The impact of reversals in wind direction between "Westerlies" and "Levanters" are shown in the Table 1.

[7] In addition to these effects, changes in the rate of formation of deep waters (WMDW) have been attributed to northwesterly wind strength, in combination with several other contributing factors, such as initial density of source waters, oceanic circulation patterns, freshwater input and greenhouse warming [*Bethoux et al.*, 1998a; *Pinardi and Masetti*, 2000; *Rohling and Bryden*, 1992]. WMDW production has been shown to be correlated with North Atlantic water evolution and the NAO index [*Rixen et al.*, 2005] or linked to strong sea to air flux promoted by local atmospheric configurations with NAO-index zero [*Lopez-Jurado et al.*, 2005].

[8] Concerning marine productivity, the Mediterranean Sea is an oligotrophic area [*Cruzado*, 1985]. However, one of the highest productivity areas is located in the Alboran basin and is associated with upwelling activity and the hydrological structure of surface waters [*Morel*, 1991]. In the open Algero Balearic basin productivity varies seasonally from mesotrophic levels due to winter convection to low productivity (oligotrophic level) during summer, linked to water column stratification [*Allen et al.*,

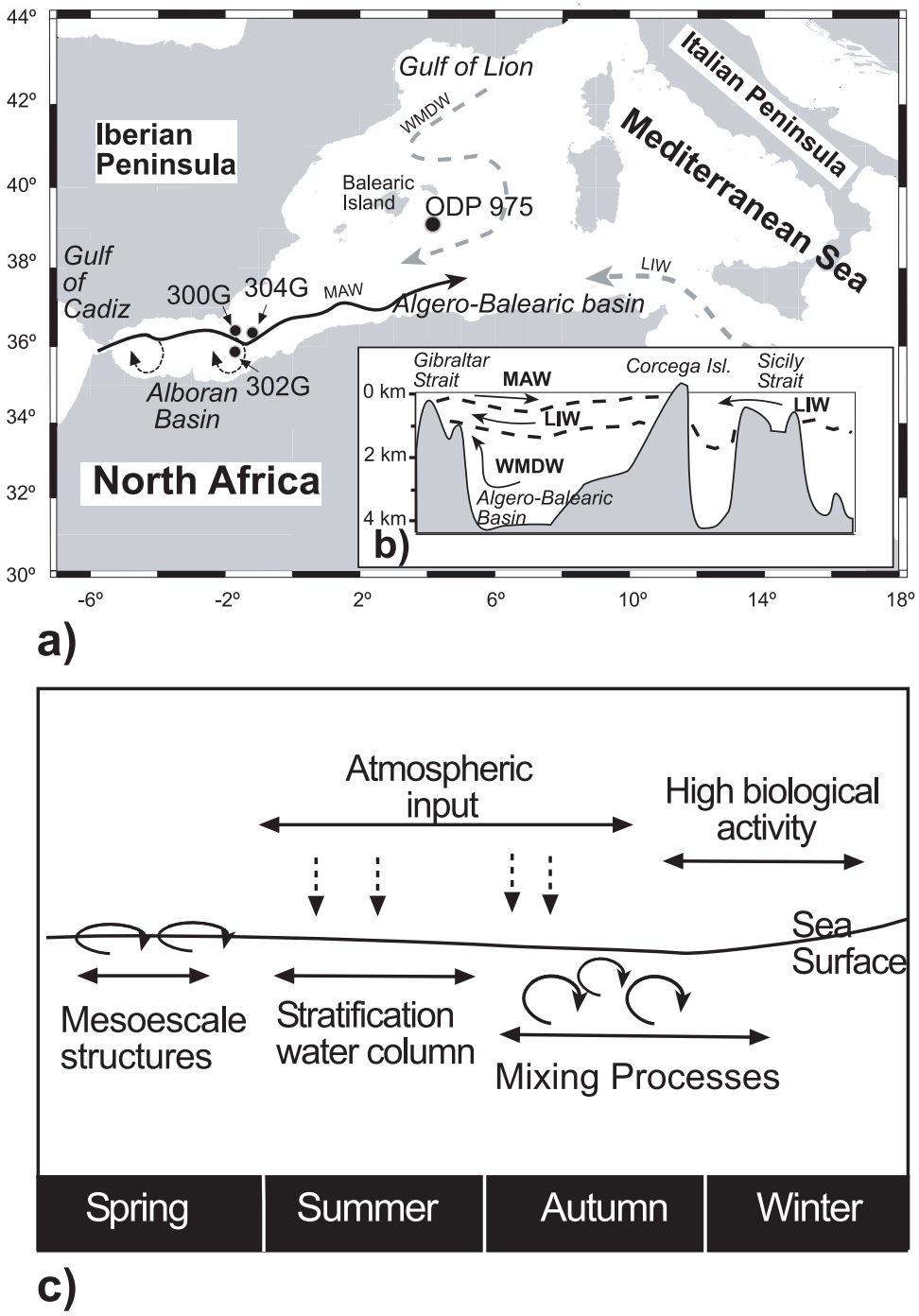

Figure 1. (a) Map of the western Mediterranean showing the location of the studied cores, TTR-300G, TTR-302G, TTR-304G, and ODP 975B. Arrows represent the main oceanographic currents. Black line indicates the Modified Atlantic Water (MAW). Black dotted lines correspond to the east and west Alboran gyres (mesoscale currents). Dashed gray lines represent the Western Mediterranean Deep Water (WMDW) and the Levantine Intermediate Water (LIW). Arrows indicate flow direction. (b) Cross section showing main water masses. Arrows indicate flow direction. Dashed black lines represent water masses boundaries. Modified from *Cramp and O'Sullivan* [1999]. (c) Schematic representation of main processes controlling water column stability and transfer of particles to the seafloor in the open Algero-Balearic basin. Modified from *Zuñiga et al.* [2008].

Table 1. Relationship Between Wind Activity and Hydrographic Conditions in the Westernmost Mediterranean Sea Based on Present Data

	$P_{Mediterranean} > P_{Atlantic}$	$P_{Atlantic} > P_{Mediterranean}$	Reference
Wind type	Levanter	Westerly	*Dorman et al.* [1995]; *Rodriguez et al.* [2001]
Flow of MAW through Gibraltar	Enhanced	Reduced	*García Lafuente et al.* [2002]
Precipitation	Reduced	Enhanced	*Dorman et al.* [1995];
Aeolian dust transportation	Enhanced	Reduced	*Rodriguez et al.* [2001]
Alboran gyre activity	Low	High	*Lampitt and Antia* [1997]
Coastal Upwelling	Off	On	

2002] (Figure 1c). Organic nutrients are brought to the WMS by Atlantic inflow [*Dafner et al.*, 2001], whereas mineral nutrients are mainly of eolian and fluvial origin, though they sometimes come from deep Mediterranean waters. Phosphate, which is mainly of fluvial origin, is the limiting nutrient for primary production in the Mediterranean Sea [*Krom et al.*, 1991; *Bethoux et al.*, 1998b].

3. Paleoenvironmental Proxies Employed

[9] The framework for interpreting planktonic stable isotope stratigraphy in general, and the framework for interpretation of $\delta^{18}O_{carbonate}$ data in the planktonic foraminifer *Globigerina bulloides* for the Iberian margin region in particular, has been well explained by different authors [e.g., *Rohling and Cooke*, 1999; *Rogerson et al.*, 2004, and references therein]. Oxygen isotope records are dominated by changes in global ice volume, but this effect can be avoided by exploring variability in the offset ($\Delta\delta^{18}O$) between cogenic isotope records from two or more locations. We exploit this concept here, by investigating $\Delta\delta^{18}O$ behavior between two synchronized records from the WMS. Furthermore, as both records are for the same species (*G. bulloides*), metabolic, seasonal and microhabitat effects on $\delta^{18}O$ can reasonably be neglected. Consequently, we interpret our $\Delta\delta^{18}O$ values as indicative of environmental gradients (temperature and freshening of surface waters) at the time of deposition. Therefore, higher temperatures and/or increases in fresh water supply will be recorded as negative excursions in the individual oxygen isotope records, and increased salinity or SST gradients between studied locations will expand $\Delta\delta^{18}O_{G.\ bulloides}$. Previous studies indicate that $\delta^{18}O_{G.\ bulloides}$ oscillations in the WMS are related mainly to changes in SST [*Cacho et al.*, 1999], freshening of the Atlantic input derived from the melting of icebergs [e.g., *Sierro et al.*, 2005], and the residence time of the Mediterranean, which is largely dependant on water depth in the Strait of Gibraltar [*Rohling*, 1999]. Though no major rivers are present within the studied area to supply excess freshwater, we also highlight that meltwater pulses from glaciers present within the surrounding mountains may be relevant if they are of significant size and share retreat timings with the better known Alpine systems [*Kerschner and Ivy-Ochs*, 2008; *Magny et al.*, 2007; *Schulte*, 2002].

[10] Carbon isotopic variability is primarily driven by the resupply of light carbon (^{12}C) to surface waters, linked with the upwelling of deep waters under particular hydrographic conditions [*Rohling and Cooke*, 1999]. A lack of ^{12}C resupply will promote heavy $\delta^{13}C_{G.\ bulloides}$ values. The major hydrographic processes in the studied region that can affect the $\delta^{13}C_{G.\ bulloides}$ signal are the presence of gyres and coastal upwelling in the Alboran Sea, changes in water column stratification (leading to changes in the depth of autumn/winter mixing) and the advection of changes in the Atlantic carbon isotopic balance due to conditions along the Portuguese Margin and in the Gulf of Cadiz [*Abrantes*, 2000; *Barcena et al.*, 2001; *Rogerson et al.*, 2004]. When cogenic records of $\delta^{13}C_{G.\ bulloides}$ are synchronized as for $\delta^{18}O$, $\Delta\delta^{13}C$ values reflect differences in productivity/upwelling between core locations. The three cores located in the Alboran basin are located eastward of the main coastal upwelling region, but their evolution is anticipated to be linked to the East Alboran gyre and the Almeria/Oran productivity front [*Sanchez-Vidal et al.*, 2005a].

[11] The sea surface water paleotemperature estimations used herein are based on the modern analog technique (MATSCH2IDW), which has already provided good results in previous studies in the area in question [e.g., *González-Donoso et al.*, 2000; *Serrano et al.*, 2007] and it is used in accordance with previous studies [*Perez-Folgado et al.*, 2003].

Table 2. Core Data Including Location, Water Depth, Studied Interval, and Linear Sedimentation Rate

Core	Location	Water Depth (m)	Studied Interval (cm)	Linear Sedimentation Rate (cm/kyr)
		Alboran Basin		
TTR14–300G	36° 21,532 N, 1° 47,507 W	1 860	55–266	13.3
TTR14–302G	36° 01,906 N, 1°57,317 W	1 989	68–335	16.75
TTR14–304G	36° 19,873 N, 1° 31,631 W	2 382	63–291	14.55
		Algero-Balearic Basin		
ODP161–975B	38°53.795′N, 4°30.596′E	2 416	31–150	7.5

[12] The use of several element/Al ratios in order to define changes in the composition of terrigenous detrital matter is based on the relationship between different minerals and their sources. This is the case for Ti/Al and Zr/Al ratios in the Mediterranean that are related to the presence of heavy minerals, mainly supplied by the Sahara aerosols [e.g., *Guieu and Thomas*, 1996], and the case of Mg/Al and K/Al ratios, in the Mediterranean Sea, where excursions in these parameters have been related with river discharge [e.g., *Frigola et al.*, 2007; *Wehausen and Brumsack*, 1998].

[13] The C/N ratio is mainly related to the balance of marine and continental organic matter in the WMS [*Kim et al.*, 2006]. Low values are typical of marine environments and high values can indicate continental influence [*Meyers*, 1994].

[14] The use of Ba as a paleoproductivity proxy has been discussed in great detail in many recent papers [e.g., *Eagle Gonneea and Paytan*, 2006, *Paytan and Griffith*, 2007, and references therein], and it has been recommended that barium proxies should be applied with caution. Barium requires enough pore water sulphate concentration to ensure the absence of sulphate reducing sediments [*Eagle et al.*, 2003; *McManus et al.*, 1998]. Moreover, Ba content is also dependent on sediment provenance, sedimentation rates, Ba cycling [*Eagle Gonneea and Paytan*, 2006; *Mercone et al.*, 2001] and lateral transport [*Fagel et al.*, 2002; *Sanchez-Vidal et al.*, 2005b].

[15] In the particular case of the westernmost Mediterranean, Ba proxies, such as the Ba/Al ratio, have been revealed to be reliable proxies [e.g., *Moreno et al.*, 2004]. No diagnetic Ba peaks have been observed which would be relatively easy to identify in the geochemical record, since they are typically high amplitude and small depth-range excursions in sedimentary barium, and thus differ from the broad Ba profiles derived from enhanced productivity. Additionally, we have also separated marine barite by sequential leaching from Ba-enriched intervals and morphological analyses of the barite crystals provide evidence for the authigenic origin of the barite crystals. In the light of this data, we consider that Ba content can be used as a reliable proxy for productivity in the WMS.

4. Studied Cores, Age Model, and Analytical Methods

4.1. Studied Cores

[16] Four cores have been analyzed (Figure 1a, Table 2) in which the interval spanning from 20 to 5 ka has been selected for this study and are shown in the auxiliary material.[1] Alboran basin cores (300G, 302G, and 304G) were collected during the Training Through Research (TTR) Cruise 14, Leg 2, while core ODP 975B-1H was recovered during the ODP Leg 161 in the Algero-Balearic basin [*Comas et al.*, 1996]. Results on this last core have been partially presented previously [*Jimenez-Espejo et al.*, 2007].

[17] Lithologies from the Alboran cores correspond to grayish olive nannofossil clay and nannofossil-rich silty clay with highly homogenous coloration. Sediments from the Algero-Balearic basin consist of nannofossil or calcareous clay, nannofossil or calcareous silty clay, and slightly bioturbated nannofossil ooze [*Comas et al.*, 1996].

4.2. Age Model

[18] The age models for the three studied cores are based on a total of 10 ^{14}C-AMS (accelerator mass spectrometry) dates measured on samples comprising monospecific planktonic foraminifers (Figures 2

[1] Auxiliary materials are available in the HTML. doi:10.1029/2008GC002096.

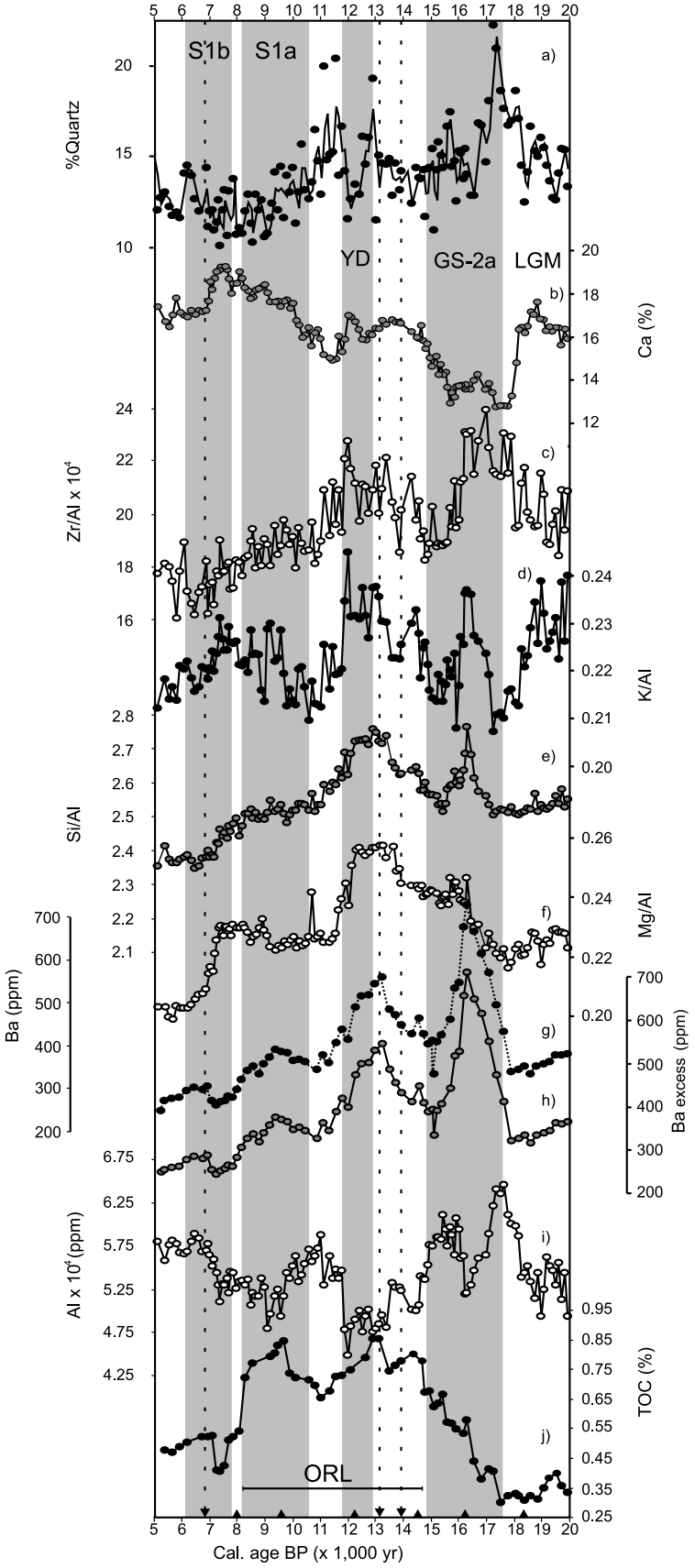
S1b
S1a
YD
GS-2a
LGM
ORL
a)
b)
c)
d)
e)
f)
g)
h)
i)
j)
%Quartz
Ca (%)
Zr/Al x 10^4
K/Al
Si/Al
Mg/Al
Ba (ppm)
Ba excess (ppm)
Al x 10^4 (ppm)
TOC (%)
Cal. age BP (x 1,000 yr)

Figure 2

and 3 and Table 3) at Leibniz-Labor for Radiometric Dating (Kiel, Germany) and Isotope Research and Poznan Radiocarbon Laboratory (Poznan, Poland). In order to compare our data with other paleoclimatic records, all ^{14}C-AMS ages were calibrated to calendar years (cal. B. P.) using the Calib 5.0 software [*Stuiver and Reimer*, 1993]. We used the MARINE04 calibration curve with the standard marine correction of 400 years that is built into the MARINE04 data [*Hughen et al.*, 2004]. The age models were verify, comparing them with other well-dated records in the WMS [*Cacho et al.*, 2001], the δ^{18}O record of the Greenland ice core GISP2 [*Grootes et al.*, 1993] (Figures 3a), NGRIP [*Lowe et al.*, 2008] and are consistent with regional sea surface isotope and SST history. Event stratigraphy timing correspond to the one proposed by the INTIMATE group (Figure 3) [*Lowe et al.*, 2008].

[19] Sedimentation rates in the Alboran basin are much higher than those estimated for the Algero-Balearic area (Table 2). Sedimentation rates in the studied Alboran sites oscillate between approximately 10 cm/ky during the Holocene and up to 20 cm/ky during some pre-Holocene periods. This study's temporal resolution is ~200 to ~50 years for Alboran sites and ~400 to ~175 years for the Algero-Balearic site.

4.3. Analytical Methods

[20] Alboran basin cores and core 975B-1H were sampled continuously in 1.5 cm and 2 cm wide intervals, respectively. Sediment samples were divided into two portions, one dried and homogenized in an agate mortar for mineralogical and geochemical analyses, the other for planktonic foraminiferal analyses.

[21] Bulk and clay mineral compositions were obtained by X-ray diffraction (XRD). Separation of the clay fraction and preparation of samples for XRD analyses were performed following the recommendations of *Kisch* [1991]. X-ray diffractograms were obtained using a Philips PW 1710 diffractometer with Cu-Kα radiation and an automatic slit. Resulting diffractograms were interpreted using Xpowder software (available at http://www.xpowder.com). Peak areas have been measured in order to estimate semiquantitative mineral content.

[22] Morphological and compositional studies of mineral phases, such as barite, were performed on selected samples by means of field emission scanning electron microscopy (FESEM, Leo Gemini1530). Quantitative geochemical microanalyses of the clay minerals were obtained by transmission electron microscopy (TEM) using a Philips CM-20 equipped with an EDAX microanalysis system.

[23] Major element measurements (Figure 2) were obtained by atomic absorption spectrometry (AAS) (Perkin-Elmer 5100 spectrometer) with an analytical error of 2% and by X-Ray Fluorescence (XRF) using a Bruker AXS S4 Pioneer.

[24] Analyses of trace elements were performed using inductively coupled plasma-mass spectrometry (ICP-MS) following HNO_3 + HF digestion. Measurements were taken in triplicates by spectrometry (Perkin-Elmer Sciex Elan 5000) using Re and Rh as internal standards. Variation coefficients determined by the dissolution of 10 replicates of powdered samples were higher than 3% and 8% for analyte concentrations of 50 ppm and 5 ppm, respectively [*Bea*, 1996].

[25] Samples from core 300G were also used to measure total organic carbon (TOC) and nitrogen. After decalcification of the samples with 6 M HCl, both were obtained by combustion at 1050°C using a Heraeus CHN-O Rapid elemental analyzer as described by *Müller et al.* [1998]. C/N (and also stable isotope) data for core 975B-1H is taken from *Jimenez-Espejo et al.* [2007].

[26] Stable carbon and oxygen isotope ratios of calcareous foraminifers from core 300G were also obtained (Figures 3b and 3c). Approximately 25 specimens of *G. bulloides* were picked from the > 125 μm fraction and senescent forms were avoided. Foraminifers were cleaned in an ultrasonic bath to remove fine-fraction contamination, rinsed with distilled water, and thoroughly washed in alcohol. Stable isotopes were measured using a Finnigan MAT 251 mass spectrometer (Isotope Laboratory, Marum, University of Bremen, Germany). All δ^{18}O data given are relative to the PDB standard. Analytical reproducibility of the method is approximately +0.07‰ for both δ^{18}O and δ^{13}C.

Figure 2. Core TTR-300G age profiles of: (a) relative quartz concentration, three-period moving average (%); (b) Ca (wt. %); (c) Zr/Al ($\times 10^4$) ratio; (d) K/Al ratio; (e) Si/Al ratio; (f) Mg/Al ratio; (g) Ba (ppm); (h) Ba_{excess} (ppm); (i) Al $\times 10^4$ (ppm); (j) Total organic carbon wt. (%) (TOC). Triangles indicate TTR-300G age model tie points. Inverted triangles and dashed black lines indicate ^{14}C dates in core TTR-300G. Black line represents the Alboran Sea basin most recent organic rich layer (ORL) time interval. LGM indicate Last Glacial Maximum time interval. Grey vertical bars indicate Greenland Stadial (GS) 2a, Younger Dryas (YD), and sapropel S1 (S1a and S1b) time intervals.

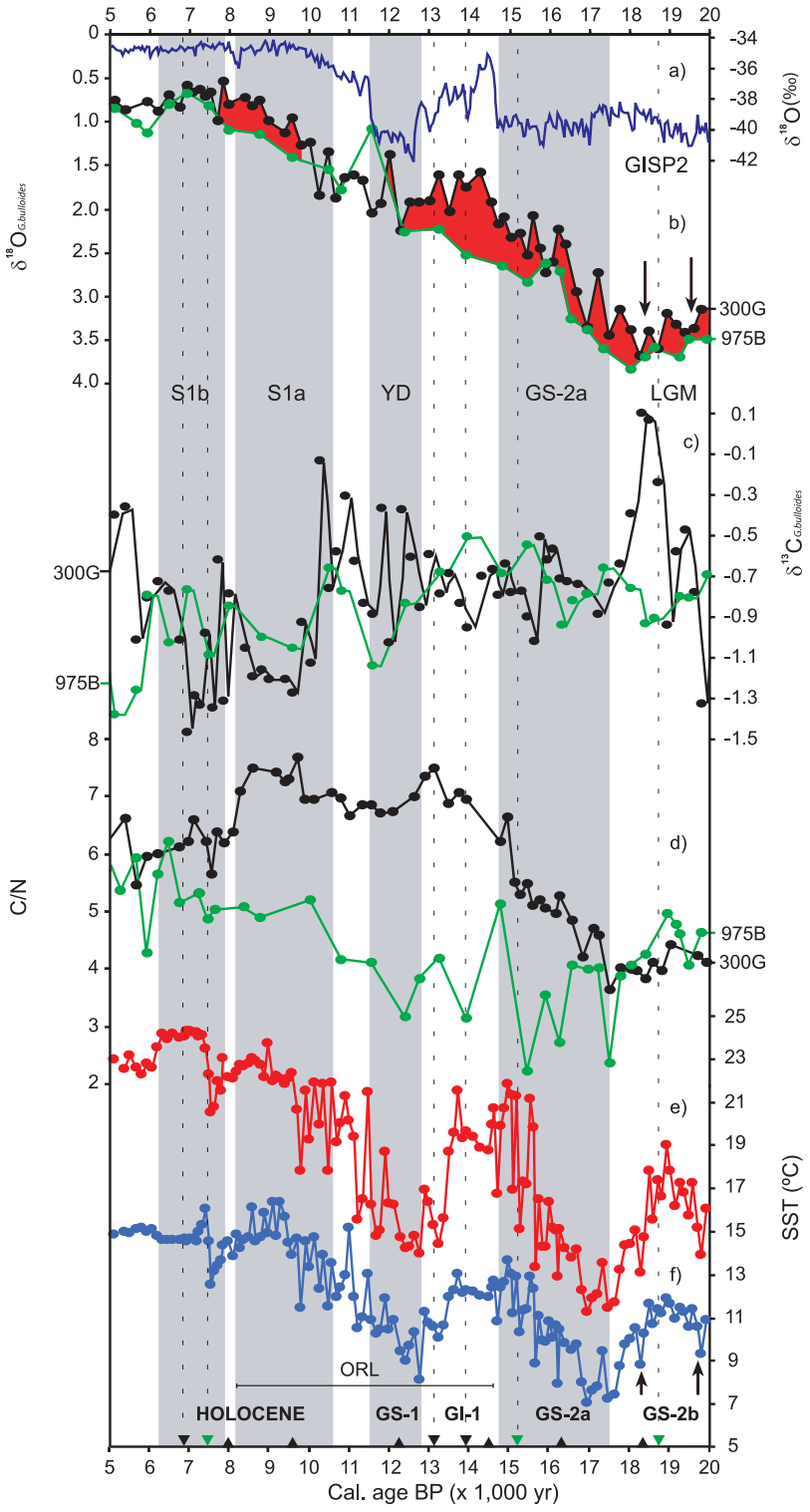
a)
GISP2
b)
300G
975B
S1b
S1a
YD
GS-2a
LGM
c)
d)
e)
f)
ORL
HOLOCENE
GS-1
GI-1
GS-2a
GS-2b
Cal. age BP (x 1,000 yr)
C/N
SST (°C)

Figure 3

Table 3. Results of AMS ^{14}C Carbon Dating of Single Planktonic *G. bulloides* (>125 μm) Taken From Cores 300G, 302G, and 975B-1H[a]

Laboratory Code	Sample Description	Core Depth, cm	Conventional Age (B. P.)	Calibrated Age (cal B. P.)[a]
Poz-14597	300G/2/17–19	75	6470 ± 40	6910 ± 80
Poz-14188	300G/3/54–56.5	168	11690 ± 60	13150 ± 65
Poz-12157	300G/4/6–7.5	179	11890 ± 60	13950 ± 65
Poz-14190	302G/5/8–10	225	11950 ± 50	13350 ± 60
Poz-14186	302G/7/53–55	374	20480 ± 100	23990 ± 160
KIA 27327	975B/1/8–10	9	2,455 + 30/ −25	2,050 ± 54
KIA 27328	975B/1/50–52	51	7,070 + 40/ −35	7,520 ± 42
KIA 27329	975B/1/90–92	91	13,330 ± 60	15,200 ± 135
KIA 27330	975B/1/130–132	131	15,870 ± 80	18,770 ± 67
KIA 27331	975B/2/45–47	190	19,460 ± 110	22,510 ± 114

[a] Calibration has been made using Calib 5.0 software. We used MARINE04 calibration curve with the standard marine correction of 400 years that is built into the MARINE04.

[27] The SST estimates for winter and summer were calculated as the mean temperature of three colder and warmer months, respectively. *González-Donoso and Linares* [1998] evaluated more than 300 modalities of TF and MAT for estimating SST values and agreed with *Dowsett and Robinson* [1997] in considering that the best results are obtained with MAT using the squared chord distance (SCD) as a measure of dissimilarity. Using this coefficient, we have selected for each core sample analyzed the ten closest core top samples of the calibration database (i.e., those that show lowest dissimilarity) and then we have calculated the mean SST value, weighting inversely the modern analogs selected as a function of their dissimilarity to the core sample. The SST associated to each sample was obtained from the archives of the National Oceanographic Data Center (NODC) [*Conkright et al.*, 2002]. For more information about calibration data set, see *Serrano et al.* [2007].

5. Results

5.1. Oxygen and Carbon Isotope and SST Variations

[28] Oxygen and carbon isotope composition (Figures 3b and 3c) has been analyzed in foraminifer separated from sediment samples from core 300G and has been compared with that of ODP 975B previously published by *Jimenez-Espejo et al.* [2007]. Maximum glacial-interglacial amplitude in the Alboran core ranges from 3.69‰ to 0.55‰ and lies between 3.84‰ and 0.69‰ for the Algero-Balearic basin, with a total oscillation of 3.14‰ and 3.15‰, respectively (Figure 3b). Although δ^{18}O shows a high correlation (r = 0.92), some discrepancies are observed between both areas. The deglacial period in both cores started at ~18 cal. ka B. P., with a continuous decreasing trend of δ^{18}O that paused during the Younger Dryas (YD). Values of δ^{18}O decrease in both basins until ~7.5 cal. ka B. P. Values of δ^{13}C are highly variable in both basins, but minimum values are reached during the Holocene (Figure 3c).

[29] Further insight on the reconstruction of past sea surface conditions was obtained from paleo-SST based in planktonic foraminifera assemblages in core TTR-300G (Figures 3e and 3f). The calculated SSTs indicate abrupt changes in surface conditions. Temperature variations of about 7°C occurred during the last deglaciation. The lowest winter SSTs (~7°C) were reached during the Greenland Stadial (GS) 2a (Figure 3f). The Bølling-Allerød (B-A) and YD are also well constrained by SST variations. Middle Holocene val-

Figure 3. Age profiles. (a) The δ^{18}O record (blue) of the Greenland ice core GISP2 [*Grootes et al.*, 1993]. (b) Offset of δ^{18}O between the *G. bulloides* in record of TTR-300G (black) and the *G. bulloides* record of ODP 975B (green), inverted scale. (c) The δ^{13}C *G. bulloides* in of TTR-300G (black) and ODP 975B (green) cores. Line corresponds to the three-period moving average, normal scale. (d) C/N ratio in of TTR-300G (black) and ODP 975B (green) cores. SST's core 300G. (e) Summer temperatures (red). (f) Winter temperatures (blue). LGM indicates Last Glacial Maximum time interval. Grey vertical bars indicate Greenland Stadial (GS) 2a, Younger Dryas (YD), and sapropel S1 (S1a and S1b) time intervals. Black line represents the Alboran Sea basin most recent organic rich layer (ORL) time interval. Arrows indicate cold water and isotopic equilibrium intrusions during the glacial period. Triangles indicate TTR-300G tie points. Inverted triangles and dashed black lines indicate ^{14}C dates in core TTR-300G (black) and core ODP 975B (green).

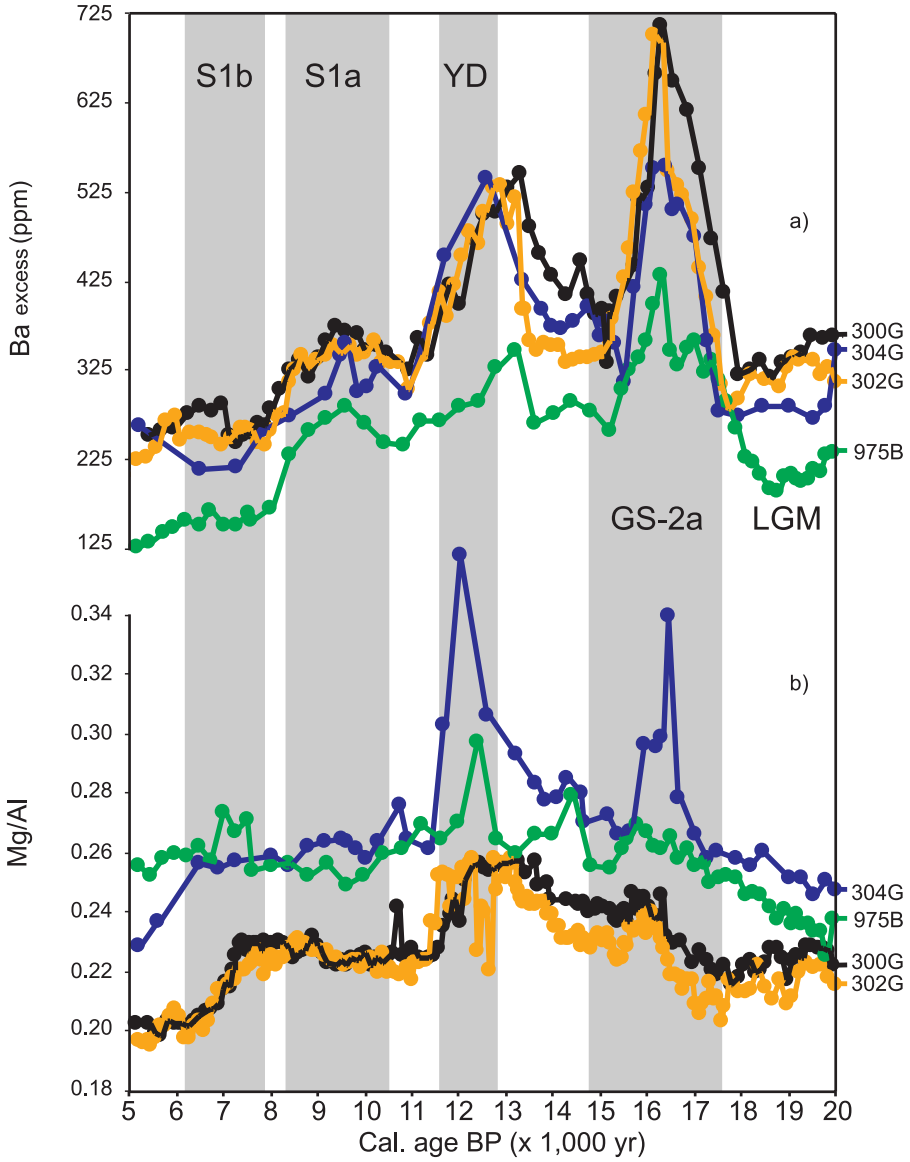

Figure 4. (a) Ba_{excess} (ppm) age plotted comparison among cores. ODP 975B values × 1.5; (b) Mg/Al ratio age plotted comparison among cores (TTR-300G: black; TTR-302G: orange; TTR-304G: blue; ODP 975B: green). LGM indicate Last Glacial Maximum time interval. Grey vertical bars indicate Greenland Stadial (GS) 2a, Younger Dryas (YD), and sapropel S1 (S1a and S1b) time intervals.

ues are marked by a highly stable pattern around 23°C for summer and 13°C for winter temperatures (Figures 3e and 3f). Those observations are in agreement with other paleo-SST records in the WMS [*Cacho et al.*, 2002; *Perez-Folgado et al.*, 2003].

5.2. Barium Excess and TOC

[30] Ba profiles from the analyzed cores are shown in Figures 2 and 4. Main Ba enrichments correspond to the middle of GS-2a and the YD onset. Sediments from these intervals have been analyzed with Field Emission Scanning Electron Microscopy (FESEM) in order to find evidence of marine barite. Barite crystals were found with sizes and morphologies corresponding to typical marine barite (1–5 μm in size with round and elliptical crystals). The Ba content derived from marine barite (Ba_{excess}) was obtained by subtracting the amount of terrigenous Ba from the total Ba content [*Dymond et al.*, 1992; *Eagle et al.*, 2003]. It is used here as the excess associated with crustal phases, and is calculated as:

$$(Ba_{excess}) = (\text{total} - Ba) - Al(Ba/Al)_{c,}$$

where total-Ba and Al are concentrations, and $(Ba/Al)_c$ is the crustal ratio for these elements. In this study, we used a value for $(Ba/Al)_c = 0.002$, as estimated by *Weldeab et al.* [2003] in the Algero-Balearic basin. For Sea Alboran cores, which have a different detrital supply, $(Ba/Al)_c = 0.0033$ was used, as estimated by *Sanchez-Vidal et al.* [2005b], on the basis of modern conditions.

[31] In spite of differences in relative amounts of Ba_{excess}, all cores show the same pattern of variations (Figure 4). Three major enrichment time intervals can be distinguished in both basins associated to the GS-2a, YD onset and early Holocene. A final minor enrichment is reached in two cores from the Alboran sea (TTR-300G and 302G) between ~7.0 and ~6.0 cal. ka B. P. (Figure 4). Highest Ba_{excess} content is observed at ~16.1 cal. ka B. P. and the lowest values are reached during the Holocene (Figure 4). TOC content is less than 0.9% at Alboran (Figure 2j) and less than 0.5% in the Algero-Balearic basin [*Jimenez-Espejo et al.*, 2007]. C_{org}/N ratios oscillate between 3.6 and 7.7 at the Alboran Sea core (Figure 3d), thus suggesting a mainly marine provenance of the organic matter [*Meyers*, 1994].

5.3. Mineralogy and Major and Trace Elements

[32] The Alboran Sea basin sediments are richer in detrital elements than the Algero-Balearic basin, and are composed of clay minerals (30–60%), calcite (25–50%), and quartz (10–20%), with low quantities of dolomite and feldspar (<5%) (Figure 2a). In all analyzed sediments, accessory minerals such as zircon, rutile, apatite, and biotite, as well as authigenic minerals, such as pyrite, Mn, and Fe oxi-hydroxides have also been identified. Clay mineral assemblages in the Algero-Balearic site consist of illite (50–80%), smectite (20–40%), and kaolinite + chlorite (15–40%) [*Jimenez-Espejo et al.*, 2007]. Clay mineral assemblage from the Alboran Sea cores are richer in illite (65–85%) and poorer in smectites (10–20%) and kaolinite + chlorite (10–25%). Additional clay minerals, such as sepiolite, palygorskite, and illite/smectite (I/S) mixed layers were identified.

[33] From the analyzed major and trace elements several records of particular interest to this study have been selected, which are shown in Figure 2. Elemental concentrations have been reduced to ratio with Al. Mg/Al and Si/Al follow a similar pattern with enrichments around 16.0 ka cal B. P. and during the YD and progressive decrease during the Holocene (Figures 2e and 2f). The K/Al ratio history is similar, but differs slightly from these detrital ratios throughout the Holocene (Figure 2d). Zr/Al ratio presents a noisy signal but does reflect changes during GS-2a and the YD.

6. Discussion

6.1. Sea Surface and Atmospheric Conditions

[34] Hydrographic survey data (MEDATLAS) indicates no significant trends in SST or salinity (and therefore no expected trend in $\Delta\delta^{18}O$) between core locations today. This is well reflected in our data, where no significant isotopic gradient ($\Delta\delta^{18}O_{G.\ bulloides}$) is found throughout the majority of the record, including the LGM and the Middle Holocene (Figure 3b). Only during the last deglaciation a persistent isotopic gradient of 1‰ is observed, thus implying that nonanalog oceanographic conditions occurred in the region between the Alboran and the Algero-Balearic basins during this period. The timing of this period of persistent gradient is significant, as it coincides with the period of deposition of the most recent Organic Rich Layer in the WMS (Figures 2j and 3b). This correlation is especially clear during TOC and gradient maximums between 14.5 to 12.5 cal. ka B. P. (B-A) and from 10 to 8 cal. ka B. P. (early Holocene) (Figures 2j and 3b). Consequently, bottom stagnation and enhanced surface gradients must be seen as both reflecting the same fundamental hydrographic change. This gradient could be driven by a strong thermal front ($\Delta\delta^{18}O = 0.5$–1‰; assuming a relationship of 0.2–0.25‰°C^{-1} [*O'Neil et al.*, 1969] this would equate to a thermal offset of 2–5°C), higher evaporation, enhanced freshwater input proximal to the Alboran Sea site or variable upward advection of ^{18}O from underlying intermediate waters between sites. The relatively short distance and open communication between basins makes evaporation an unlikely explanation, and a front of this magnitude would be anticipated to be accompanied by a significant change in the planktonic foraminiferal assemblage, typically high abundance of *Globorotalia inflata* [*Rohling et al.*, 1995], and this is not observed. Furthermore, the small catchment areas of rivers feeding the Alboran Sea make fresh water influence, riverine derived, unlikely to sustain the observed isotopic offset. Consequently, upward advection of ^{18}O from intermediate water seems the most probable explanation for this offset.

[35] Enhanced vertical mixing in the Alboran basin surface water during the deglaciation indicates a less stable water column compared to the middle Holocene or the LGM. Vertical stability is controlled by a number of factors, but primarily the vertical density and velocity gradients. Recent work concerning the origin of the most recent WMS Organic Rich Layer emphasizes the role of shoaling of the WMS deep circulation during this period [*Rogerson et al.*, 2008]. This would increase the westward velocity of intermediate waters and thus increase the shear between surface and intermediate waters. Consequently, turbulence will be increased promoting vertical mixing in the Alboran basin, thus driving an offset in $\Delta\delta^{18}O$ in the WMS. A further consequence of this enhanced vertical mixing would be increased resupply of nutrients to the surface (see below).

[36] Although the middle-Holocene and LGM both represent periods of low $\Delta\delta^{18}O$ values, they follow different trends (Figure 3b). During the LGM, cold spells are consistent with periods of ~0 $\Delta\delta^{18}O$ values and peaks in $\Delta\delta^{13}C$ (Arrows Figures 3b, 3c, and 3f). These observations suggest variable ^{12}C resupply that can be promoted by upwelling intensification in the Alboran basin or enhanced advection of Atlantic-derived carbon during these cold phases. These observations thus indicate strong westerly winds and low pressures in the WMS, which will promote intense upwelling development within the gyres positioned to the west of the Alboran Sea core site and/or intensified Atlantic jet inflow while maintaining low (i.e., modern-like) $\Delta\delta^{18}O$ (i.e., strong vertical stratification) between the basins (Table 1).

[37] Among these cold periods, the middle of the GS-2a presents several distinctive features. Simultaneous decrease in $\Delta\delta^{18}O$ and $\Delta\delta^{13}C$ indicates very strong water column stratification, sufficient even to suppress upwelling west of the Alboran Sea core sites (Figures 3b and 3c). This is coincident with high aeolian input (inferred from high Zr/Al ratio; Figure 2c), implicating persistent "Levanter" type wind conditions [cf. *Bout-Roumazeilles et al.*, 2007]. The middle of the GS-2a (16.3 to 15.9 ka cal B. P.) is a very interesting period for the WMS, and major hydrographic changes are known to have occurred. At this time, a significant freshening in the WMS sea surface, related to fresher Atlantic input and North Atlantic iceberg melting, has been described [*Sierro et al.*, 2005]. This freshening promoted a major thermohaline change and reduced bottom ventilation, a consequence of enhanced buoyancy of surface water [e.g., *Cacho et al.*, 2000; *Sierro et al.*, 2005]. Our data, coincident with these observations, confirm the presence of a highly stable water column ($\Delta\delta^{18}O$ and $\Delta\delta^{13}C \sim 0$; Figures 3b and 3c) at this time. However, there is no strong difference between late and early GS-2a, implicating strong stratification throughout this period.

[38] During the YD, dry and cold conditions were re-established in the WMS region [*Barcena et al.*, 2001; *González-Sampériz et al.*, 2008]. $\Delta\delta^{18}O$ follows a flat pattern in both basins and during the YD the $\Delta\delta^{18}O$ offset disappears (Figure 3b). Values of $\delta^{13}C$ become very unstable in the Alboran basin during the YD, presumably reflecting a complex hydrographic setting until 10 cal. ka B. P. (Figure 3c). From the end of the YD, a new situation is observed in the WMS. Dramatic SST oscillations occurred involving a sharp warming contemporary with the Termination 1B, especially during summer, (>5°C in less than 200 years) (Figure 3e), and at ~11.5 cal. ka B. P. a marked $\delta^{18}O$ peak occurred in both basins, with the Algero-Balearic values exceptionally exceeding those from the Alboran basin (Figure 3b). This implies a minor inverted isotopic gradient to the early deglaciation that could reflect a high temperature contrast and/or increase in the fresh water input in the Algero-Balearic area. The latter case may be related to the successive ice cap retreats that took place in west-central Europe, from which meltwater water would be supplied to the WMS via the Rhone, around 11.5 cal. ka B. P. [*Magny et al.*, 2007].

[39] During the early Holocene (10.0 to ~8.0 cal. ka B. P., coincident with the final phase of Organic Rich Layer 1), a minor oxygen isotope offset between both areas is evident, with the Alboran Sea again showing lighter $\delta^{18}O$ values. This period shows a stable pattern in SST as well as in other proxies and low $\delta^{13}C$ in the Alboran basin. The weak oxygen isotopic gradient may reflect freshening of the Alboran Sea or, as with the early deglacial, somewhat enhanced vertical mixing. During this period, wet conditions have been described in different continental records in the WMS [*Frisia et al.*, 2006; *Zanchetta et al.*, 2007], as well as a minimum in bottom ventilation conditions in the Algero-Balearic basin [*Jimenez-Espejo et al.*, 2007]. Low aeolian input (Figure 2c) during this period confirms the generally humid conditions. These conditions ended between ~7.7 and ~7.2 cal. ka B. P., when a major oceanographic

change occurred, giving rise to the modern setting of eddies and frontal circulation patterns of the WMS [*Perez-Folgado et al.*, 2003; *Rohling et al.*, 1995]. After ~7.2 cal. ka B. P., minor or no $\Delta\delta^{18}O$ offset is reached between basins, highly variable $\delta^{13}C$, well oxygenated bottom waters and steady SST values reflecting the present hydrographical pattern [*Rohling et al.*, 1995].

6.2. Paleoproductivity Conditions

[40] During the LGM the low C/N values in both basins indicate a marine origin for TOC and minor terrestrial input (Figure 3d). The high Ba_{excess} values in the Alboran Sea and strong productivity offset between basins indicate that upwelling in the Alboran region and continental margin influence were the main control of productivity gradients in the WMS (Figure 4a).

[41] Productivity during the GS-2a, as reflected by Ba-based proxies, was high throughout the entire event, with a maximum peak at the middle (Figure 4a). The increase in the eolian input during this period (Figure 2c) may have promoted certain degree of fertilization in surface water, as has been observed in the present during "red rain" events [*Sarthou and Jeandel*, 2001], but the required aeolian input flux seems unrealistic to explain the entire productivity anomaly [*Krom et al.*, 2005]. High $\delta^{13}C$ in the Alboran Sea is argued to reflect reduced upwelling (see above), making hydrographic enhancement of productivity also unlikely (Figure 3c). Consequently, enhanced nutrient flux must reflect enhanced flux of relatively fertilized Atlantic surface water.

[42] At the middle of the GS-2a we observed the highest Ba_{excess} contents reached at the same time as surface freshening reaches its peak in the western and central Mediterranean Sea [*Sierro et al.*, 2005]. TOC and Ba_{excess} follow a different pattern during this interval, and apparently TOC "burning" by reoxigenation fronts are absent during the GS-2a (Figures 2h and 2j). Recent studies of coastal northwest Africa have linked Ba increases with meltwater pulses via dissolved Ba input via the Azores Front and changes in the Ba/Al_c ratio during the GS-2a period [*Plewa et al.*, 2006]. The close proximity of the Alboran Sea to this region and the known contribution of water from the Azores Current to the Gibraltar inflow [*Özgökmen et al.*, 2001] suggest that dissolved Ba could have potentially affected Ba profiles in the Alboran Sea. Moreover, this middle GS-2a high productivity is coincident with a peak in Mg/Al (Figures 2f and 2h and Figures 4a and 4b), indicating incursion of exotic material (e.g., detrital carbonates, rich Mg-Chlorites).

[43] We obtain high-to-moderate correlation values through the entire studied interval between Ba_{excess} and Mg/Al in the Alboran Sea (Figures 2f, 2g, and 2h) during certain time intervals (r = between 0.534 to 0.804), but no correlation in the Algero-Balearic basin (r = 0.039). This observation can be interpreted in two ways: similar input source for Ba and Mg or a link between Mg sources and productivity as during the middle GS-2a. Ba enriched iceberg meltwater [*Plewa et al.*, 2006] loaded with detrital Mg-bearing carbonates could have also occurred, as well as increase in the terrestrial weathering during this reduced-vegetation period [e.g., *Carrión and Van Geel*, 1999; *Schulte et al.*, 2008], both phenomena can promote surface water fertilization or simply increase Ba and Mg contents. Nevertheless, performed semiquantitative XRD mineralogical analyses do not allow to distinguish major variations in dolomite or chlorite because of the small variations in their content relative to analytical error (5–10%). Further studies and analysis of Ba-carrier phases could shed light on the magnitude of this exotic influence, although presence of marine barite in sediments from this interval provides evidence for enhanced productivity.

[44] Ba_{excess} is consistently higher during the deglacial than during either the LGM or the Holocene, including the B-A which presents a local minimum, and displays a series of short-term peaks (Figure 4a). This period is coincident with the period of pronounced $\Delta\delta^{18}O$ (Figure 3b) and is also associated with a coetaneous increase in the C/N ratio in the Alboran basin (Figure 3d). A certain degree of fluvial or continental shelf material influence may be the cause of the shift in the C/N ratio. However, it should also be noted that this period is at the height of the period of Organic Rich Layer deposition (Figure 2j). Nutricline doming, due to shoaling of deep circulation [*Rogerson et al.*, 2008], is therefore also implicated for this rise in Ba_{excess}, which is consistent with arguments presented for the origin of the $\Delta\delta^{18}O$ expansion during this time.

[45] The beginning of the YD is marked by a significant increase in Ba_{excess}, which is more pronounced in the Alboran Sea basin (Figure 4a). No major changes are observed in the WMS hydrography; however, different conditions occurred compared to during to the middle of the GS-2a [*Bard et al.*, 2000] and Ba enriched iceberg

meltwater is not expected [*Plewa et al.*, 2006]. Previous studies based on diatoms indicate relatively low levels of salinity in surface waters, related to a decrease in salt content of the Atlantic input and increased local river activity in the Alboran margin [*Barcena et al.*, 2001]. In this sense high Mg/Al ratios in both basins and high C/N offset suggest the influence of fluvial activity (Figures 3d and 4b), despite arid continental conditions prevailing at that time (Figure 2c) [e.g., *Carrión and Van Geel*, 1999; *Bar-Matthews et al.*, 2003; *González-Sampériz et al.*, 2008]. This apparent contradiction can be explained by a combination of reduced sediment supply and increased sediment transport rate [*Schulte et al.*, 2008]. In this sense, increase of torrential rainstorms with increased runoff during drier climate episodes in the Mediterranean littoral has been described in subrecent periods [*Barriendos and Martin-Vide*, 1998]. During the YD travertine crisis [e.g., *Martin-Algarra et al.*, 2003] and major river incision event has been described in the South Iberian region [*Schulte et al.*, 2008]. The transferred sediment, funneled through rivers and canyons, could bypass the pronounced slope reaching the marine basin, increasing Mg/Al ratio and an initiating submarine-fan system [*Lo Iacono et al.*, 2008]. The absence of pronounced Mg/Al peak in two of the Alboran cores (Figure 4b) can indicate a minor influence of these locations to the funneled sediments. On the other hand, glacier retreat/advance in the Betics/Rif mountain chains, increasing freshwater supply, is expectable during the YD [*Schulte*, 2002], nevertheless the lack of absolute dates in the surrounding mountain chains make this observation an untested hypothesis. Either or both of these processes may have supplied additional nutrients and kept productivity relatively high in the narrow Alboran basin but at lower levels than during established $\Delta\delta^{18}O$ conditions.

[46] Along the YD and Holocene onset (12.5 to 10 cal. ka B. P.) ORL and Ba_{excess} content reached a relative minimum peak in coincidence with no $\Delta\delta^{18}O$ (Figures 2h, 2j, 3b, and 4a). Only after 10 cal. ka B. P. (early Holocene) TOC and Ba_{excess} reached again relatively high contents in both basins, compared with middle Holocene and LGM values. This period coincides with warmer, wetter climatic conditions in the Mediterranean and changes in Ba_{excess} appear to coincide with the last Sapropel deposit evolution in the Eastern Mediterranean (Figures 3e and 4a) [*Ariztegui et al.*, 2000; *Martinez-Ruiz et al.*, 2003]. A major drop in marine productivity occurred around 8.2 cal. ka B. P. reflected in both proxies (Figures 2j and 4a), when cold, dry conditions recurred throughout the northern hemisphere [e.g., *Alley and Agustsdottir*, 2005]. These observations confirm some degree of linkage between WMS productivity, water column stability and atmospheric conditions, as would be expected from the regional climatology (Table 1).

[47] Additional evidence of connection between atmospheric conditions and marine productivity is reflected in the aeolian and fluvial input. Aeolian input appears to be very low during early Holocene, as indicated by low Zr/Al ratio (Figure 2c), and this concept is consistent with evidence of wet conditions registered in central WMS records [*Frisia et al.*, 2006; *Zanchetta et al.*, 2007]. The Mg/Al did not undergo major variations during these dry events but the major decrease around ~7 cal ka B. P. (Figures 2f and 4b) can be associate with the end of the African Humid Period [e.g., *deMenocal et al.*, 2000; *Swezey*, 2001; *Liu et al.*, 2007].

7. Conclusions

[48] Sea surface temperatures, oxygen isotope values, and geochemical proxies indicate significant climate and oceanographic variations in the westernmost Mediterranean Sea since the LGM. Cold spells during the LGM have been described and related with upwelling intensification and/or Atlantic derived carbon advection forced by intense westerly winds. A C/N and isotopic offset between studied WMS basins has been recognized, as well as, parallel productivity oscillations. Thus we present two different scenarios associated to the isotopic gradient in the WMS: (1) during established isotopic gradient periods, Bølling-Allerød and early Holocene, when warm conditions, an unstable water column, enhanced productivity and low bottom oxygen conditions appear to have been reached; (2) no $\Delta\delta^{18}O$ gradient, analog to present conditions (more stable water column and low marine productivity) occurred during the LGM and from ~8.0 cal. ka B. P. Decoupling between productivity proxies, TOC and Ba, during the GS-2a had been discussed and a possible external Ba source not discarded. The isotopic values reached in the Algero-Balearic basin at 11.5 cal. ka B. P. should indicate a possible glacial meltwater influence. Additionally, riverine influence has been described based on the Mg/Al ratio which suffers a major fall around 7 cal ka B. P. probably associated to the end of the African Humid Period.

A "bypass" process, that could increase sediment transport to the marine basin in spite drier conditions, has been proposed in order to explain Mg/Al peaks during arid periods such as middle GS-2a and Younger Dryas.

Acknowledgments

[49] This work was financed by project CGL2006-13327-C04-04 (MEC), project RNM 432 and Research Group RNM 179 (Junta de Andalucía) and Postdoctoral Research Fellow of the Japan Society for the Promotion of Science (JSPS). We also thank projects CSD2006–00041 (TOPOIBERIA) and CSD2007–00067 (GRACCIE) and the European Access to Research Infrastructures (ARI) Paleostudies grant. Special thanks to IMAGES/PAGES workshop on Circum-Iberia Palaeoceanography and Palaeoclimate. This research used samples and/or data provided by the Ocean Drilling Program (ODP). ODP is sponsored by the U.S. National Science Foundation (NSF) and participating countries under management of Joint Oceanographic Institutions (JOI), Inc. We would like to thank the ODP Core Repository (Bremen, Germany) for their assistance with sampling, and the University of Bremen for the use of the XRF core scanner. Other geochemical analyses were performed at the "Centro de Instrumentación Científica" (University of Granada), the Department of Mineralogy and Petrology (University of Granada), Bremen University, and the Japan Agency for Marine-Earth and Science Technology (JAMSTEC) laboratories. The authors are indebted to A.H.L. Voelker as coeditor and to A. Asioli and one anonymous reviewer for their invaluable comments and reviews. MR thanks the Hull Environmental Research Institute for their support. Our thanks to K. Iijima, E. Abarca, E. Holanda, J. Montes, C. Niembro, and D. Ortega for their laboratory assistance.

References

Abrantes, F. (2000), 200,000 yr diatom records from Atlantic upwelling sites reveal maximum productivity during LGM and a shift in phytoplankton community structure at 185,000 yr, *Earth Planet. Sci. Lett.*, *176*, 7–16, doi:10.1016/S0012-821X(99)00312-X.

Allen, J. I., P. J. Somerfield, and J. Siddorn (2002), Primary and bacterial production in the Mediterranean Sea: A modelling study, *J. Mar. Syst.*, *33–34*, 473–495, doi:10.1016/S0924-7963(02)00072-6.

Alley, R. B., and A. M. Agustsdottir (2005), The 8k event: Cause and consequences of a major Holocene abrupt climate change, *Quat. Sci. Rev.*, *24*, 1123–1149, doi:10.1016/j.quascirev.2004.12.004.

Ariztegui, D., A. Asioli, J. Lowe, F. Trincardi, L. Vigliotti, F. Tamburini, C. Chondrogianni, A. Accorsi, M. Bandini Mazzanti, and A. M. Mercuri (2000), Palaeoclimate and the formation of sapropel S1: Inferences from Late Quaternary lacustrine and marine sequences in the central Mediterranean region, *Palaeogeogr. Palaeoclimatol. Palaeoecol.*, *158*, 215–240, doi:10.1016/S0031-0182(00)00051-1.

Bar-Matthews, M., A. Ayalon, M. Gilmour, A. Matthews, and J. Hawkesworth (2003), Sea-land oxygen isotopic relationships from planktonic foraminifera and speleothems in the Eastern Mediterranean region and their implication for paleorainfall during interglacial intervals, *Geochim. Cosmochim. Acta*, *67*, 3181–3199, doi:10.1016/S0016-7037(02)01031-1.

Barcena, M. A., I. Cacho, F. Abrantes, F. J. Sierro, J. O. Grimalt, and J. A. Flores (2001), Paleoproductivity variations related to climatic conditions in the Alboran Sea (western Mediterranean) during the last glacial-interglacial transition: The diatom record, *Palaeogeogr. Palaeoclimatol. Palaeoecol.*, *167*, 337–357, doi:10.1016/S0031-0182(00)00246-7.

Bard, E., F. Rostek, J.-L. Turon, and S. Gendreau (2000), Hydrological impact of Heinrich Events in the Subtropical Northeast Atlantic, *Science*, *289*, 1321–1324, doi:10.1126/science.289.5483.1321.

Barriendos, M., and J. Martin-Vide (1998), Secular climatic oscillations as indicated by catastrophic floods in the Spanish Mediterranean coastal area (14th–19th centuries), *Clim. Change*, *38*, 473–491.

Bea, F. (1996), Residence of REE, Y, Th and U in granites and crustal protoliths: Implications for the chemistry of crustal melts, *J. Petrol.*, *37*, 521–532, doi:10.1093/petrology/37.3.521.

Benzohra, M., and C. Millot (1995), Characteristics and circulation of the surface and intermediate water masses off Algeria, *Deep Sea Res. Part I*, *42*, 1803–1830, doi:10.1016/0967-0637(95)00043-6.

Bethoux, J., B. Gentili, and D. Tailliez (1998a), Warming and freshwater budget change in the Mediterranean since the 1940s, their possible relation to the greenhouse effect, *Geophys. Res. Lett.*, *25*, 1023–1026, doi:10.1029/98GL00724.

Bethoux, J. P., C. Morin, C. Chaumery, O. Connon, B. Gentili, and D. Ruiz-Pino (1998b), Nutrients in the Mediterranean Sea, mass balance and statistical analysis of concentrations with respect to environmental change, *Mar. Chem.*, *63*, 155–169, doi:10.1016/S0304-4203(98)00059-0.

Bout-Roumazeilles, V., N. Combourieu Nebout, O. Peyron, E. Cortijo, A. Landais, and V. Masson-Delmotte (2007), Connection between South Mediterranean climate and North African atmospheric circulation during the last 50000 yr BP North Atlantic cold events, *Quat. Sci. Rev.*, *26*, 3197–3215, doi:10.1016/j.quascirev.2007.07.015.

Bryden, H. L., and H. M. Stommel (1982), Origins of the Mediterranean Outflow, *J. Mar. Res.*, *40*, 55–71.

Bucca, P. J., and T. H. Kinder (1984), An example of meteorological effects on the Alboran Sea Gyre, *J. Geophys. Res.*, *89*, 751–757, doi:10.1029/JC089iC01p00751.

Cacho, I., J. O. Grimalt, C. Pelejero, M. Canals, F. J. Sierro, A. Flores, and N. J. Shackleton (1999), Dansgaard-Oeschger and Heinrich event imprints in Alboran Sea temperatures, *Paleoceanography*, *14*, 698–705, doi:10.1029/1999PA900044.

Cacho, I., O. Grimalt, J. Sierro, J. Shackleton, and M. Canals (2000), Evidence for enhanced Mediterranean thermohaline circulation during rapid climatic coolings, *Earth Planet. Sci. Lett.*, *183*, 417–429, doi:10.1016/S0012-821X(00)00296-X.

Cacho, I., O. Grimalt, M. Canals, L. Sbaffi, J. Shackleton, J. Schonfeld, and R. Zahn (2001), Variability of the Western Mediterranean sea-surface temperature during the last 25000 years and its connection with the Northern-Hemisphere climatic changes, *Paleoceanography*, *16*, 40–52, doi:10.1029/2000PA000502.

Cacho, I., O. Grimalt, and M. Canals (2002), Response of the western Mediterranean Sea to rapid climatic variability during the last 50,000 years: A molecular biomarker

approach, *J. Mar. Syst.*, *33–34*, 253–272, doi:10.1016/S0924-7963(02)00061-1.

Cacho, I., N. Shackleton, H. Elderfield, F. J. Sierro, and J. O. Grimalt (2006), Glacial rapid variability in deep-water temperature and ä^{18}O from the Western Mediterranean Sea, *Quat. Sci. Rev.*, *25*, 3294–3311, doi:10.1016/j.quascirev.2006.10.004.

Carrión, J. S., and B. Van Geel (1999), Fine-resolution Upper Weichselian and Holocene palynological record from Navarrés (Valencia, Spain) and a discussion about factors of Mediterranean forest succession, *Rev. Palaeobot. Palynol.*, *106*, 209–236, doi:10.1016/S0034-6667(99)00009-3.

Colmenero-Hidalgo, E., J.-A. Flores, F. J. Sierro, A. Bárcena, L. Löwemark, J. Schönfeld, and J. O. Grimalt (2004), Ocean surface water response to short-term climate changes revealed by coccolithophores from the Gulf of Cadiz (NE Atlantic) and Alboran Sea (W Mediterranean), *Palaeogeogr. Palaeoclimatol. Palaeoecol.*, *205*, 317–336, doi:10.1016/j.palaeo.2003.12.014.

Comas, M. C., et al. (1996), *Proceedings of Ocean Drilling Program, Initial Reports161*, Ocean Drill. Program, College Station, Tex.

Conkright, M. E., R. A. Locarnini, H. E. García, T. D. O'Brien, T. P. Boyer, C. Stephens, and J. I. Antonov(2002), *World Ocean Atlas 2001: Objective Analyses, Data Statistics, and Figures, CD-ROM Documentation*, Natl. Oceanogr. Data Cent., Silver Spring, Md.

Cramp, A., and G. O'Sullivan (1999), Neogene sapropels in the Mediterranean: A review, *Mar. Geol.*, *153*, 11–28, doi:10.1016/S0025-3227(98)00092-9.

Cruzado, A. (1985), Chemistry of Mediterranean Waters, in *Western Mediterranean*, edited by R. Margalef, pp. 126–147, Pergamon, Oxford, U.K.

Dafner, E. V., R. Sempere, and H. L. Bryden (2001), Total organic carbon distribution and budget through the Strait of Gibraltar in April 1998, *Mar. Chem.*, *73*, 233–252, doi:10.1016/S0304-4203(00)00109-2.

de Menocal, P. D., J. Ortiz, T. Guilderson, and M. Sarnthein (2000), Coherent high-and low-latitude climate variability during the Holocene warm period, *Science*, *288*, 2198–2202, doi:10.1126/science.288.5474.2198.

Dorman, C. E., R. C. Beardsley, and R Limeburner (1995), Winds in the Strait of Gibraltar, *Q. J. R. Meteorol. Soc.*, *121*, 1903–1921, doi:10.1002/qj.49712152807.

Dowsett, H. J., and M. M. Robinson (1997), Application of the modern analogs technique (MAT) of sea surface temperature estimation to middle Pliocene North Pacific planktonic foraminifer assemblages, *Palaeontol. Electron.*, *1*. (Available at http://palaeo-electronica.org/1998_1/dowsett/issue1.htm)

Dymond, J., E. Suess, and J. M. Lyle (1992), Barium in deep-sea sediment: A geochemical proxy for paleoproductivity, *Paleoceanography*, *7*, 163–181, doi:10.1029/92PA00181.

Eagle, M., A. Paytan, K. Arrigo, G. Van Dijken, and R. Murray (2003), A comparison between excess Barium and Barite as indicators or export production, *Paleoceanography*, *18*(1), 1021, doi:10.1029/2002PA000793.

Eagle Gonneea, M., and A. Paytan (2006), Phase associations of barium in marine sediments, *Mar. Chem.*, *100*, 124–135, doi:10.1016/j.marchem.2005.12.003.

Emeis, K. C., U. Struck, H. M. Schulz, R. Rosenberg, S. Bernasconi, H. Erlenkeuser, T. Sakamoto, and F. Martinez-Ruiz (2000), Temperature and salinity variations of Mediterranean Sea surface waters over the last 16000 years from records of planktonic stable oxygen isotopes and alkenone unsaturation ratios, *Palaeogeogr. Palaeoclimatol. Palaeoecol.*, *158*, 259–280, doi:10.1016/S0031-0182(00)00053-5.

Fagel, N., F. Dehairs, L. André, G. Bareille, and C. Monnin (2002), Export production estimation from sedimentary Ba content: A comparison between Atlantic and Indian sectors of the Southern Ocean, *Paleoceanography*, *17*(2), 1011, doi:10.1029/2000PA000552.

Frigola, J., A. Moreno, I. Cacho, M. Canals, J. Sierro, A. Flores, J. O. Grimalt, D. A. Hodell, and J. H. Curtis (2007), Holocene climate variability in the western Mediterranean region from a deepwater sediment record, *Paleoceanography*, *22*, PA2209, doi:10.1029/2006PA001307.

Frisia, S., A. Borsato, A. Mangini, C. Spötl, G. Madonia, and U. Sauro (2006), Holocene climate variability from a discontinuous stalagmite record and the Mesolithic to Neolithic transition, *Quat. Res.*, *66*, 388–400, doi:10.1016/j.yqres.2006.05.003.

García Lafuente, J., J. Delgado, M. Vargas, M. Vargas, F. Plaza, and T. Sarhan (2002), Low frequency variability of the exchanged flows through the Strait of Gibraltar during CANIGO, *Deep Sea Res., Part II*, *49*, 4051–4067, doi:10.1016/S0967-0645(02)00142-X.

González-Donoso, J. M., and D. Linares (1998), Evaluation of some numerical techniques for determining paleotemperatures from planktonic foraminiferal assemblages, *Rev. Esp. Paleontol.*, *13*, 107–129.

González-Donoso, J. M., F. Serrano, and D. Linares (2000), Sea surface temperature during the Quaternary at ODP Sites 976 and 975(western Mediterranean), *Palaeogeogr. Palaeoclimatol. Palaeoecol.*, *162*, 17–44, doi:10.1016/S0031-0182(00)00103-6.

González-Sampériz, P., L. Valero-Garces, A. Moreno, M. Morellón, A. Navas, J. Machín, and A. Delgado-Huertas (2008), Vegetation changes and hydrological fluctuations in the Central Ebro Basin (NE Spain) since the Late Glacial period: Saline lake records, *Palaeogeogr. Palaeoclimatol. Palaeoecol.*, *259*, 157–181, doi:10.1016/j.palaeo.2007.10.005.

Grootes, P. M., M. Stuiver, J. W. C. White, S. Johnsen, and J. Jouzel (1993), Comparison of oxygen isotope records from the GISP2 and GRIP Greenland ice cores, *Nature*, *366*, 552–554, doi:10.1038/366552a0.

Guieu, C., and A. Thomas (1996), Saharan aerosol: From the soil to the ocean, in *The Impact of Desert Dust Across the Mediterranean*, edited by S. Guerzoni and R. Chester, pp. 207–216, Kluwer Acad., Dordrecht, Netherlands.

Hughen, K., et al. (2004), Marine04: Marine radiocarbon age calibration, 26–0 ka BP, *Radiocarbon*, *46*, 1059–1086.

Jimenez-Espejo, F. J., F. Martinez-Ruiz, T. Sakamoto, K. Iijima, D. Gallego-Torres, and N. Harada (2007), Paleonvironmental changes in the western Mediterranean since the last glacial maximum: High resolution multiproxy record from the Algero-Balearic basin, *Palaeogeogr. Palaeoclimatol. Palaeoecol.*, *246*, 292–306, doi:10.1016/j.palaeo.2006.10.005.

Kerschner, H., and S. Ivy-Ochs (2008), Palaeoclimate from glaciers: Examples from the Eastern Alps during the Alpine Lateglacial and early Holocene, *Global Planet. Change*, *60*(1), 58–71.

Kim, J.-H., S. Schouten, R. Buscail, W. Ludwig, J. Bonnin, S. Sinninghe Damste, and F. Bourrin (2006), Origin and distribution of terrestrial organic matter in the NW Mediterranean (Gulf of Lions): Exploring the newly developed BIT index, *Geochem. Geophys. Geosyst.*, *7*, Q11017, doi:10.1029/2006GC001306.

Kisch, H. J. (1991), Illite crystalinity: Recommendations on sample preparation, X-ray diffraction settings, and interlaboratory samples, *J. Metamorph. Geol.*, *9*, 665–670, doi:10.1111/j.1525-1314.1991.tb00556.x.

Krijgsman, W. (2002), The Mediterranean: Mare Nostrum of earth sciences, *Earth Planet. Sci. Lett.*, *205*(1–12), doi:10.1016/S0012-821X(02)01008-7.

Krom, M. D., S. Brenner, N. Kress, and L. I. Gordon (1991), Phosphorus limitation of primary productivity in the E. Mediterranean Sea, *Limnol. Oceanogr.*, *36*, 424–432.

Krom, M. D., et al. (2005), Summary and overview of the CYCLOPS P addition Lagrangian experiment in the Eastern Mediterranean, *Deep Sea Res., Part II*, *52*, 3090–3108, doi:10.1016/j.dsr2.2005.08.018.

Lampitt, R. S., and A. N. Antia (1997), Particle flux in Deep Seas: Regional characteristics and temporal variability, *Deep Sea Res. Part I*, *44*, 1377–1403, doi:10.1016/S0967-0637(97)00020-4.

Liquete, C., P. Arnau, M. Canals, and S. Colas (2005), Mediterranean river systems of Andalusia, southern Spain, and associated deltas: A source to sink approach: Mediterranean Prodelta Systems*Mar. Geol.*, *222–223*, 471–495, doi:10.1016/j.margeo.2005.06.033.

Liu, Z., et al. (2007), Simulating the transient evolution and abrupt change of Northern Africa atmosphere-ocean-terrestrial ecosystem in the Holocene, *Quat. Sci. Rev.*, *26*, 1818–1837, doi:10.1016/j.quascirev.2007.03.002.

Llave, E., J. Schönfeld, F. J. Hernández-Molina, T. Mulder, L. Somoza, V. DíazdelRío, and I. Sánchez-Almazo (2006), High-resolution stratigraphy of the Mediterranean outflow contourite system in the Gulf of Cadiz during the late Pleistocene: The impact of Heinrich events, *Mar. Geol.*, *227*, 241–262, doi:10.1016/j.margeo.2005.11.015.

Lobo, F. J., L. M. Fernandez-Salas, I. Moreno, J. L. Sanz, and A. Maldonado (2006), The sea-floor morphology of a Mediterranean shelf fed by small rivers, northern Alboran Sea margin, *Cont. Shelf Res.*, *26*, 2607–2628, doi:10.1016/j.csr.2006.08.006.

Lo Iacono, C., E. Gràcia, S. Diez, G. Bozzano, X. Moreno, J. Dañobeitia, and B. Alonso (2008), Seafloor characterization and backscatter variability of the Almería Margin (Alboran Sea, SW Mediterranean) based on high-resolution acoustic data, *Mar. Geol.*, *250*(1–18), doi:10.1016/j.margeo.2007.11.004.

Lopez-Jurado, J., C. Gonzalez-Pola, and P. Velez-Belchi (2005), Observation of an abrupt disruption of the long-term warming trend at the Balearic Sea, western Mediterranean Sea, in summer 2005, *Geophys. Res. Lett.*, *32*, L24606, doi:10.1029/2005GL024430.

Lowe, J. J., S. O. Rasmussen, S. Bjoerck, W. Z. Hoek, J. P. Steffensen, M. J. C. Walker, Z. C. Yu, and INTIMATE group (2008), Synchronisation of palaeoenvironmental events in the North Atlantic region during the Last Termination: A revised protocol recommended by the INTIMATE group, *Quat. Sci. Rev.*, *27*, 6–17, doi:10.1016/j.quascirev.2007.09.016.

Macías, D., M. Bruno, F. Echevarría, A. Vázquez, and C. M. García (2008), Meteorologically induced mesoscale variability of the North-western Alboran Sea (Southern Spain) and related biological patterns, *Estuarine Coastal Shelf Sci.*, *78*, 250–266, doi:10.1016/j.ecss.2007.12.008.

Magny, M., et al. (2007), Holocene climate changes in the central Mediterranean as recorded by lake-level fluctuations at Lake Accesa (Tuscany, Italy), *Quat. Sci. Rev.*, *26*, 1736–1758, doi:10.1016/j.quascirev.2007.04.014.

Martin-Algarra, A., M. Martín-Martín, B. Andreo, R. Juliá, and C. González-Perez (2003), Sedientary patterns in perched spring travertines near Granada (Spain) as indicators of the paleohydrological and paleoclmatological evolution of a karst massif, *Sediment. Geol.*, *161*, 217–228, doi:10.1016/S0037-0738(03)00115-5.

Martinez-Ruiz, F., A. Paytan, M. Kastner, J. M. Gonzalez-Donoso, D. Linares, S. M. Bernasconi, and F. J. Jimenez-Espejo (2003), A comparative study of the geochemical and mineralogical characteristics of the S1 sapropel in the western and eastern Mediterranean, *Palaeogeogr. Palaeoclimatol. Palaeoecol.*, *190*, 23–37, doi:10.1016/S0031-0182(02)00597-7.

Martrat, B., J. O. Grimalt, C. Lopez-Martinez, I. Cacho, F. J. Sierro, J. A. Flores, R. Zahn, M. Canals, J. H. Curtis, and D. A. Hodell (2004), Abrupt temperature changes in the Western Mediterranean over the past 250000 years, *Science*, *306*, 1762–1765, doi:10.1126/science.1101706.

McManus, J., W. M. Berelson, G. P. Klinkhammer, K. S. Johnson, K. H. Coale, R. F. Anderson, N. Kumar, D. J. Burdige, D. E. Hammond, and H. J. Brumsack (1998), Geochemistry of barium in marine sediments: Implications for its use as a paleoproxy, *Geochim. Cosmochim. Acta*, *62*, 3453–3473, doi:10.1016/S0016-7037(98)00248-8.

Mercone, D., J. Thomson, R. H. Abu-Zied, I. W. Croudace, and E. J. Rohling (2001), High-resolution geochemical and micropalaeontological profiling of the most recent eastern Mediterranean sapropel, *Mar. Geol.*, *177*, 25–44, doi:10.1016/S0025-3227(01)00122-0.

Meyers, P. A. (1994), Preservation of elemental and isotopic source identification of sedimentary organic matter, *Chem. Geol.*, *114*, 289–302, doi:10.1016/0009-2541(94)90059-0.

Millot, C. (1987), Circulation in the Western Mediterranean-Sea, *Oceanol. Acta*, *10*, 143–149.

Millot, C. (1999), Circulation in the western Mediterranean Sea, *J. Mar. Syst.*, *20*, 423–442, doi:10.1016/S0924-7963(98)00078-5.

Morel, A. (1991), Light and marine photosynthesis: A spectral model with geochemical and climatological implications, *Prog. Oceanogr.*, *26*, 263–306, doi:10.1016/0079-6611(91)90004-6.

Moreno, A., I. Cacho, M. Canals, J. O. Grimalt, and A. Sanchez-Vidal (2004), Millennial-scale variability in the productivity signal from the Alboran Sea record, Western Mediterranean Sea, *Palaeogeogr. Palaeoclimatol. Palaeoecol.*, *211*, 205–219, doi:10.1016/j.palaeo.2004.05.007.

Moreno, A., I. Cacho, M. Canals, J. O. Grimalt, M. F. Sánchez-Goñi, N. Shackleton, and F. J. Sierro (2005), Links between marine and atmospheric processes oscillating on a millennial time-scale. A multi-proxy study of the last 50000 yr from the Alboran Sea (Western Mediterranean Sea). Quaternary land-ocean correlation, *Quat. Sci. Rev.*, *24*, 1623–1636, doi:10.1016/j.quascirev.2004.06.018.

Müller, P. J., G. Kirst, G. Ruhland, I. vonStorch, and A. Rosell-Mele (1998), Calibration of the alkenone paleotemperature index Uk'37 based on core-tops form the eastern South Atlantic and the global ocean (60°N-60°S), *Geochim. Cosmochim. Acta*, *62*, 1757–1772, doi:10.1016/S0016-7037(98)00097-0.

O'Neil, J. R., et al. (1969), Oxygen isotope fractionation on divalent metal carbonates, *J. Chem. Phys.*, *51*, 5547–5558, doi:10.1063/1.1671982.

Özgökmen, T. M., E. P. Chassignet, and C. G. H. Rooth (2001), On the connection between the Mediterranean Outflow and the Azores current, *J. Phys. Oceanogr.*, *31*, 461–480, doi:10.1175/1520-0485(2001)031<0461:OTCBTM>2.0.CO;2.

Paytan, A., and E. M. Griffith (2007), Marine barite: Recorder of variations in ocean export productivity, *Deep Sea Res.*, *54*, 687–705.

Perez-Folgado, M., F. J. Sierro, J. A. Flores, I. Cacho, J. O. Grimalt, R. Zahn, and N. Shackleton (2003), Western Mediterranean planktonic foraminifera events and millennial climatic variability during the last 70 kyr, *Mar. Micropaleontol.*, *48*, 49–70, doi:10.1016/S0377-8398(02)00160-3.

Pinardi, N., and E. Masetti (2000), Variability of the large scale general circulation of the Mediterranean Sea from observations and modelling: A review, *Palaeogeogr. Palaeoclimatol. Palaeoecol.*, *158*, 153–173, doi:10.1016/S0031-0182(00)00048-1.

Plewa, K., H. Meggers, and S. Kasten (2006), Barium in sediments off northwest Africa: A tracer for paleoproductivity or meltwaters events?, *Paleoceanography*, *21*, PA2015, doi:10.1029/2005PA001136.

Rixen, T., M. V. S. Guptha, and V. Ittekkot (2005), Deep ocean fluxes and their link to surface ocean processes and the biological pump, *Prog. Oceanogr.*, *65*, 240–259, doi:10.1016/j.pocean.2005.03.006.

Rodriguez, S., X. Querol, A. Alastuey, G. Kallos, and O. Kakaliagou (2001), Saharan dust contributions to PM10 and TSP levels in Southern and Eastern Spain, *Atmos. Environ.*, *35*, 2433–2447, doi:10.1016/S1352-2310(00)00496-9.

Rogerson, M., E. J. Rohling, P. P. E. Weaver, and J. W. Murray (2004), The Azores Front since the Last Glacial Maximum, *Earth Planet. Sci. Lett.*, *222*, 779–789, doi:10.1016/j.epsl.2004.03.039.

Rogerson, M., J. Rohling, P. P. E. Weaver, and J. W. Murray (2005), Glacial to interglacial changes in the settling depth of the Mediterranean Outflow plume, *Paleoceanography*, *20*, PA3007, doi:10.1029/2004PA001106.

Rogerson, M., E. J. Rohling, and P. P. E. Weaver (2006), Promotion of meridional overturning by Mediterranean-derived salt during the last deglaciation, *Paleoceanography*, *21*, PA4101, doi:10.1029/2006PA001306.

Rogerson, M., I. Cacho, F. J. Jimenez-Espejo, M. I. Reguera, F. J. Sierro, F. Martinez-Ruiz, J. Frigola, and M. Canals (2008), A dinamic explanation for the origin of the Western Mediterranean organic rich layers, *Geochem. Geophys. Geosyst.*, *9*, Q07U01, doi:10.1029/2007GC001936.

Rohling, E. J. (1999), Environmental control on Mediterranean salinity and delta O-18, *Paleoceanography*, *14*, 706–715, doi:10.1029/1999PA900042.

Rohling, E. J., and H. L. Bryden (1992), Man-induced salinity and temperature increases in western Mediterranean deep water, *J. Geophys. Res.*, *97*, 11,191–11,198, doi:10.1029/92JC00767.

Rohling, E. J. and S. Cooke (1999), Stable oxygen and carbon isotope ratios in foraminiferal carbonate shells, in *Modern Foraminifera*, edited by B. K. Sen Gupta, pp. 239–258, Kluwer Acad., Dordrecht, Netherlands.

Rohling, E., M. Den Dulk, C. Pujol, and C. Vergnaud-Grazzini (1995), Abrupt hydrographic change in the Alboran Sea (western Mediterranean) around 8000 yrs BP, *Deep Sea Res., Part I*, *42*, 1609–1619, doi:10.1016/0967-0637(95)00069-I.

Sanchez-Vidal, A., A. Calafat, M. Canals, J. Frigola, and J. Fabres (2005a), Particle fluxes and organic carbon balance across the Eastern Alboran Sea (SW Mediterranean Sea), *Cont. Shelf Res.*, *25*, 609–628, doi:10.1016/j.csr.2004.11.004.

Sanchez-Vidal, A., R. W. Collier, A. Calafat, J. Fabres, and M. Canals (2005b), Particulate barium fluxes on the continental margin: A study from the Alboran Sea (Western Mediterranean), *Mar. Chem.*, *93*, 105–117, doi:10.1016/j.marchem.2004.07.004.

Sarthou, G., and C. Jeandel (2001), Seasonal variations of iron concentrations in the Ligurian Sea and iron budget in the Western Mediterranean, *Mar. Chem.*, *74*, 115–129, doi:10.1016/S0304-4203(00)00119-5.

Schulte, L. (2002), Climatic and human influence on river systems and glacier fluctuations in southeast Spain since the Last Glacial Maximum, *Quat. Int.*, *93–94*, 85–100, doi:10.1016/S1040-6182(02)00008-3.

Schulte, L., R. Julia, F. Burjachs, and A. Hilgers (2008), Middle Pleistocene to Holocene geochronology of the River Aguas terrace sequence (Iberian Peninsula): Fluvial response to Mediterranean environmental change, *Geomorphology*, *98*, 13–33, doi:10.1016/j.geomorph.2007.03.018.

Serrano, F. J., J. M. González-Donoso, P. Palmqvist, A. Guerra-Merchán, D. Linares, and J. A. Pérez-Claros (2007), Estimating Pliocene sea-surface temperatures in the Mediterranean: An approach based on the modern analogs technique, *Palaeogeogr. Palaeoclimatol. Palaeoecol.*, *243*, 174–188, doi:10.1016/j.palaeo.2006.07.012.

Sierro, F. J., et al. (2005), Impact of iceberg melting on Mediterranean thermohaline circulation during Heinrich events, *Paleoceanography*, *20*, PA2019, doi:10.1029/2004PA001051.

Stuiver, M., and P. J. Reimer (1993), Extended ^{14}C data base and revised CALIB 3.0 14C Age calibration program, *Radiocarbon*, *35*, 215–230.

Swezey, C. (2001), Eolian sediment responses to late Quaternary climate changes: Temporal and spatial patterns in the Sahara, *Palaeogeogr. Palaeoclimatol. Palaeoecol.*, *167*, 119–155, doi:10.1016/S0031-0182(00)00235-2.

Voelker, A. H. L., S. M. Lebreiro, J. Schönfeld, I. Cacho, H. Erlenkeuser, and F. Abrantes (2006), Mediterranean outflow strengthening during northern hemisphere coolings: A salt source for the glacial Atlantic?, *Earth Planet. Sci. Lett.*, *245*, 39–55, doi:10.1016/j.epsl.2006.03.014.

Wehausen, R., and H. J. Brumsack (1998), The formation of Pliocene Mediterranean sapropels: Constraints from high-resolution major and minor elements studies, *Proc. Ocean Drill. Program Sci. Results*, *160*, 207–218.

Weldeab, S., W. Siebel, R. Wehausen, K.-C. Emeis, G. Schmiedl, and C. Hemleben (2003), Late Pleistocene Western Mediterranean Sea: Implications for productivity changes and climatic conditions in the catchment areas, *Palaeogeogr. Palaeoclimatol. Palaeoecol.*, *190*, 121–137, doi:10.1016/S0031-0182(02)00602-8.

Zanchetta, G., R. N. Drysdale, J. C. Hellstrom, A. E. Fallick, I. Isola, M. K. Gagan, and M. T. Pareschi (2007), Enhanced rainfall in the Western Mediterranean during deposition of sapropel S1: Stalagmite evidence from Corchia cave (Central Italy), *Quat. Sci. Rev.*, *26*, 279–286, doi:10.1016/j.quascirev.2006.12.003.

Zuñiga, D., et al. (2008), Compositional and temporal evolution of particle fluxes in the open Algero-Balearic basin (Western Mediterranean), *J. Mar. Syst.*, *70*, 196–214, doi:10.1016/j.jmarsys.2007.05.007.